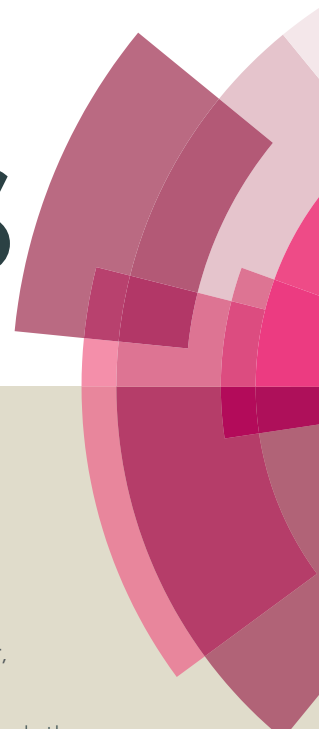


RSC Advances



This article can be cited before page numbers have been issued, to do this please use: M. Esmailpour, A. Sardarian, A. Jarrahpour, E. Ebrahimi and J. javidi, *RSC Adv.*, 2016, DOI: 10.1039/C6RA03634A.



This is an *Accepted Manuscript*, which has been through the Royal Society of Chemistry peer review process and has been accepted for publication.

Accepted Manuscripts are published online shortly after acceptance, before technical editing, formatting and proof reading. Using this free service, authors can make their results available to the community, in citable form, before we publish the edited article. This *Accepted Manuscript* will be replaced by the edited, formatted and paginated article as soon as this is available.

You can find more information about *Accepted Manuscripts* in the [Information for Authors](#).

Please note that technical editing may introduce minor changes to the text and/or graphics, which may alter content. The journal's standard [Terms & Conditions](#) and the [Ethical guidelines](#) still apply. In no event shall the Royal Society of Chemistry be held responsible for any errors or omissions in this *Accepted Manuscript* or any consequences arising from the use of any information it contains.

Synthesis and characterization of β -lactam functionalized superparamagnetic $\text{Fe}_3\text{O}_4@\text{SiO}_2$ nanoparticles as an approach for improvement of antibacterial activity of β -lactams

Mohsen Esmailpour⁽¹⁾, Ali Reza Sardarian^{(1)*}, Aliasghar Jarrahpour⁽¹⁾, Edris Ebrahimi⁽¹⁾, Jaber Javidi^(2,3)

(1) Chemistry Department, College of Sciences, Shiraz University, Shiraz, Iran

(2) Department of Pharmaceutics, School of Pharmacy, Shahid Beheshti University of Medical Sciences, Tehran, Iran

(3) Students Research Committee, School of Pharmacy, Shahid Beheshti University of Medical Sciences, Tehran, Iran

*Corresponding author. Tel.: +98 7116137107, fax: +98 7112286008.

E-mail addresses: asardarian55@shirazu.ac.ir (A.R. Sardarian)

Abstract

In this paper, we reported, for the first time, a new multistep method for preparing β -lactam functionalized $\text{Fe}_3\text{O}_4@\text{SiO}_2$ nanoparticles with high saturation magnetization. The synthesized nanostructures were characterized by FT-IR, XRD, TEM, FE-SEM, TGA, DLS, N_2 adsorption-desorption isotherm analysis, elemental analysis, NMR and Mass spectroscopy. Also, the magnetic property of these Fe_3O_4 nanoparticles allowed simple separation of these nanoparticles from the reaction mixture by an external magnetic field. β -Lactams (**2a-f**) and nano $\text{Fe}_3\text{O}_4@\text{SiO}_2/\beta$ -lactams (**3a-f**) were tested against Gram-positive *S. aureus* (ATCC 25923) and Gram-negative *Escherichia coli* (ATCC 25922) and results showed the minimum inhibitory concentrations (MICs) of **3a-f** were less than **2a-f**.

Keywords:

β -Lactam; [2+2] Cycloaddition; Core-shell; $\text{Fe}_3\text{O}_4@\text{SiO}_2$; Superparamagnetism; Antibacterial activity

1. Introduction

Invasive all bacterial, fungal and viral infections are a serious and escalating health issue. Current therapies are limited in safety and resistant fungi, bacteria, and viruses are an emerging problem.¹ It is widely recognized that there is a need for the optimization of pharmacological properties or development of new drugs that have a different mode of action to those currently in use.²

β -Lactam antibiotics have played an important role in antibacterial drugs and in medicinal chemistry.³⁻⁵ β -Lactams are not only useful fragments of antibiotics, but are also used as intermediates and synthons for the production of several organic compounds.⁶⁻⁹ They have been widely used as chemotherapeutic agents for treating microbial diseases.¹⁰⁻¹¹ They also show many other interesting biological properties, such as anti-HIV,¹² anti malarial activities,¹³ antitumor,¹⁴ anti-hyperglycemic,¹⁵ anti-

inflammatory, analgesic activities,¹⁶ cholesterol absorption inhibitors,¹⁷ thrombin inhibitors,¹⁸ serine-dependent enzyme inhibitors¹⁹ and human cytomegalovirus protease inhibitors.²⁰ Due to importance of β -lactams several synthetic methods have been developed for the preparation of the β -lactam ring²¹⁻²⁵ and among the several methods, the [2+2] cycloaddition reaction of Schiff bases with ketenes (Staudinger reaction) is mostly applied.²⁶ The ketenes are commonly generated in situ from acyl halides or activate carboxylic acids in the presence of tertiary amines.²⁷⁻²⁹ The activate carboxylic acids are conventionally useful when the acid halides are not commercially available, difficult to prepare or when they are unstable.³⁰ Some acid activating agents include trifluoroacetic anhydride,³¹ tri-phosgene,³² cyanuric chloride,³³ 1,1-carbonyldi-imidazole,³⁴ phosphorus-derived reagents,³⁵ acetic anhydride,³⁶ Mukaiyama reagent³⁷ and thionyl chloride (or oxalyl chloride).³⁸

Nanomedicine as drug delivery vehicles have been designed and synthesized that can carry drug and efficiently cross physiological membranes to reach target sites.³⁹ The most representative nanoscale carriers include gold nanoparticles,⁴⁰ liposomes,⁴¹ quantum dots,⁴² magnetic nanoparticles,⁴³ polymeric nanoparticles,⁴⁴ carbon nanotubes,⁴⁵ engineered viral nanoparticles,⁴⁶ nucleic acid-based nanoconstructs⁴⁷ and dendrimers.⁴⁸

In last decades, magnetic nanoparticles have attracted much attention because of their unique physio-chemical properties and potential applications such as medical diagnostics and therapeutics,^{49,50} data storage,⁵¹ environmental remediation,⁵² magnetic resonance imaging (MRI)^{53,54} and catalysis.⁵⁵

Because of biological restrictions, such as avoiding toxic materials or using sufficiently low frequencies and field amplitudes to prevent the formation of eddy currents inside the patient's body, several papers have focused on magnetic nanostructures,⁵⁶⁻⁵⁸ in particular, magnetite Fe_3O_4 nanoparticles. These nanoparticles have shown significant attractive for the preparation of immobilized derivative penicillin G, cephalosporin and amoxicillin because of the easy and complete separation from the reaction mixture by applying a magnetic field.⁵⁹⁻⁶¹ Using magnetite nanosystems have been investigated to improve the efficiency of current antimicrobials with proved effect.⁶²

For many applications, magnetic nanoparticles are suitable to be chemically stable and uniform in size to prevent their aggregation, which is happened due to their nanoscale and strong interaction among them. This problem can be solved by coating of magnetite nanoparticles with a silica layer as the stabilizer, which prevents direct contact between the nanoparticles. Furthermore, it provides the abound hydroxyl groups on the surface of composite particles and the opportunity to conjugate various function molecules for many special applications.^{63,64}

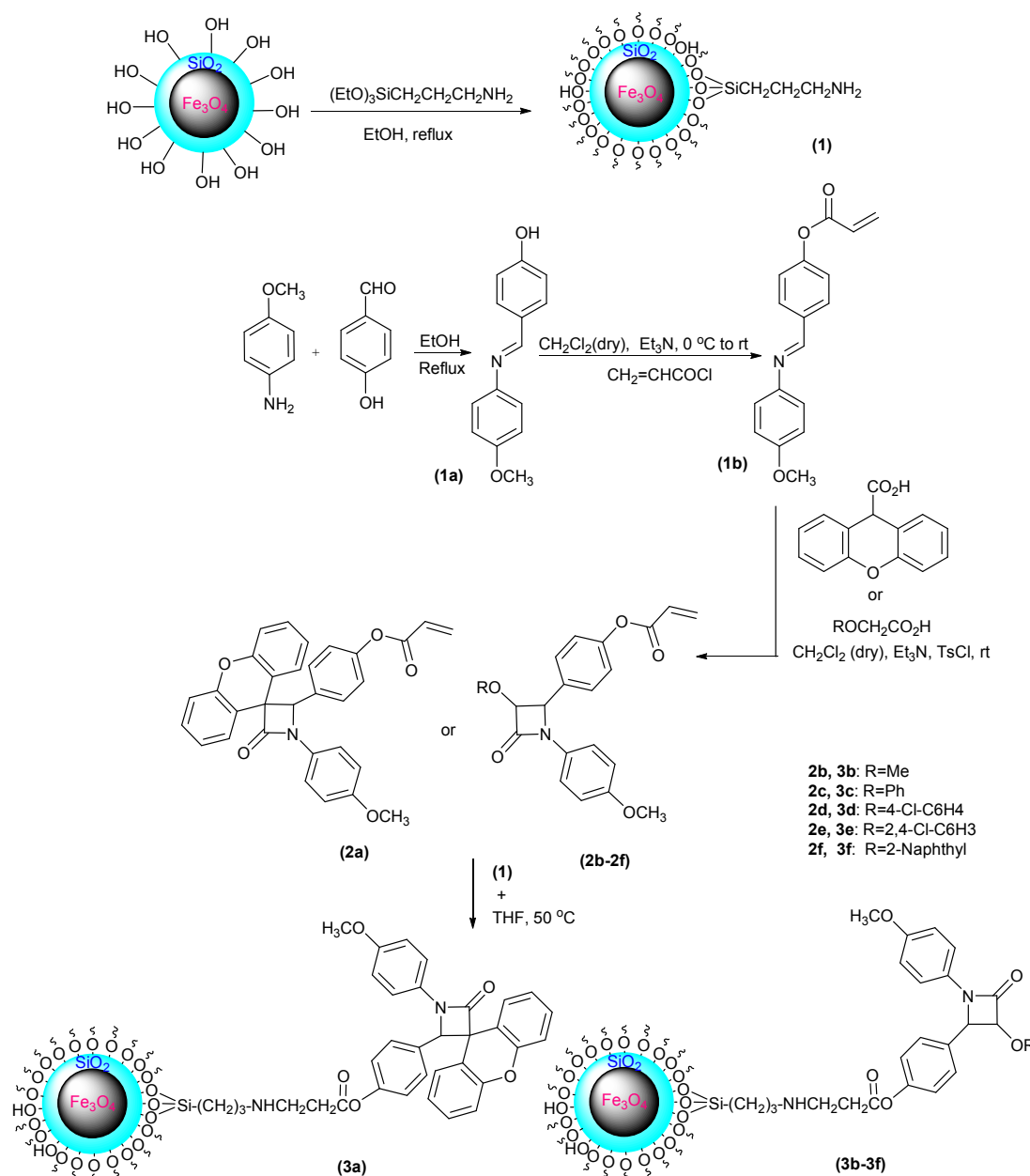
Recently, magnetic core-shell materials have gained much attention and undergone intensive investigation for their unique potential applications in medicinal, low cytotoxicity, chemically modifiable surface, magnetic responsively, good stability, optical, biological, environmental and chemical areas.^{65,66} On the other hand, core-shell nanostructure magnetic catalysts could be easily separated conveniently and economically using an external magnetic field.⁶⁶

Therefore, regarding to the previous report on the synthesis of functionalized iron nanoparticles-penicillin conjugates to combat the rapid emergence of β -lactamase resistance,⁶⁷ we decided, herein to use Fe_3O_4 nanoparticles, which have high saturation magnetization, for preparation of β -lactam functionalized $\text{Fe}_3\text{O}_4@\text{SiO}_2$ nanoparticles and then characterize their structure and properties by different techniques such as FT-IR, XRD, TEM, FE-SEM, TGA, DLS, N_2 adsorption-desorption isotherm analysis, elemental analysis, NMR and Mass spectroscopy. Finally, the antibacterial activity of β -lactam (**2a-f**) and β -lactam functionalized $\text{Fe}_3\text{O}_4@\text{SiO}_2$ nanoparticles (**3a-f**) were tested against gram-positive *S. aureus* (ATCC 25923) and gram-negative *Escherichia coli* (ATCC 25922) bacterial strain.

2. Results and discussion

2.1. Characterization of β -lactam functionalized $\text{Fe}_3\text{O}_4@\text{SiO}_2$ nanoparticles

In this paper, the synthesis of β -lactam functionalized $\text{Fe}_3\text{O}_4@\text{SiO}_2$ nanoparticles are reported for the first time to the best of our knowledge on the basis of the reactions presented in Scheme 1.



Scheme 1. Process for preparation of β -lactam functionalized $\text{Fe}_3\text{O}_4@\text{SiO}_2$ nanoparticles.

Acrylated- β -lactams **2a-f** were synthesized from acrylated-Schiff base **1b** and acetic acid derivatives. For synthesis of Schiff base **1a** a mixture of 4-methoxyaniline and 4-hydroxybenzaldehyde was refluxed in ethanol. In the next step acrylated-Schiff base **1b** was achieved from Schiff base **1a** and acryloyl chloride in the presence of Et_3N in dry CH_2Cl_2 at 0°C to room temperature. The acrylated-Schiff base **1b** was used to synthesize acrylated- β -lactams **2a-f** by modified [2+2] ketene-imine cycloaddition reactions (Staudinger) in the presence of *p*-toluenesulfonyl chloride and Et_3N in dry CH_2Cl_2 at room temperature. The acrylated- β -lactams **2a-f** were characterized by spectral analyses. The *cis* and *trans* stereochemistry of 2-azetidinones were realized

from the coupling constants of H-3 and H-4 ($J_{3,4} > 4.0$ Hz for the *cis* and $J_{3,4} < 3.0$ Hz for the *trans* stereoisomer).⁶⁸

As a model, IR spectrum of **2c** showed a sharp band at 1762 cm^{-1} for the β -lactam carbonyl which is a proof of the β -lactam ring and absorption at 1682 cm^{-1} for the carbonyl of the acrylate. The $^1\text{H-NMR}$ spectrum of **2c** displayed two doublets for H-3 and H-4 of β -lactam ring at 5.55 ppm (d, $J = 4.70$, 1H) and 5.36 ppm (d, $J = 4.70$, 1H), respectively. The detected coupling constants of these protons established the *cis* stereochemistry for this compound. The $^{13}\text{C-NMR}$ spectrum of compound **2c** showed the β -lactam carbonyl peak at 164.1 ppm. In addition, the carbon of methoxy group, C-4 and C-3 of β -lactam ring appeared at 55.4, 61.4 and 81.1 ppm, respectively.

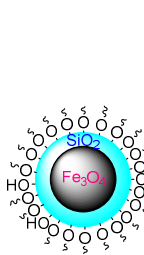
Magnetic nanoparticles coated by 3-(triethoxysilyl)-propylamine ($\text{Fe}_3\text{O}_4@\text{SiO}_2\text{-NH}_2$) (**1**) was prepared by addition of 3-(triethoxysilyl)-propylamine to dispersed powder of $\text{Fe}_3\text{O}_4@\text{SiO}_2$ in ethanol. After 12h reflux, suspension of $\text{Fe}_3\text{O}_4@\text{SiO}_2\text{-NH}_2$ was separated with the external magnetic field, washed with ethanol and water and dried at $80\text{ }^\circ\text{C}$.

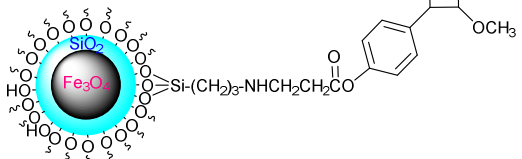
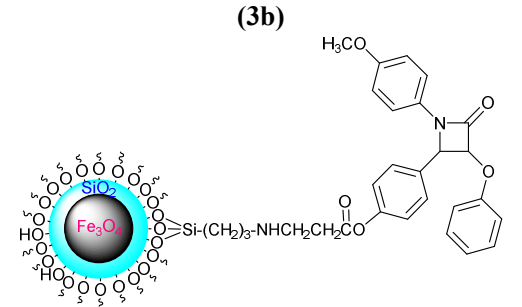
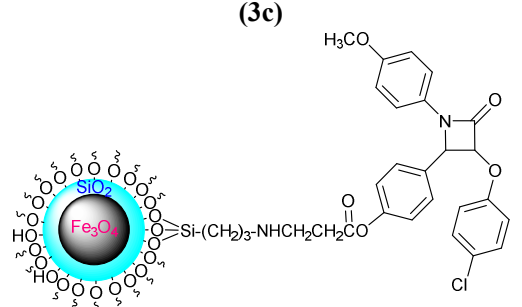
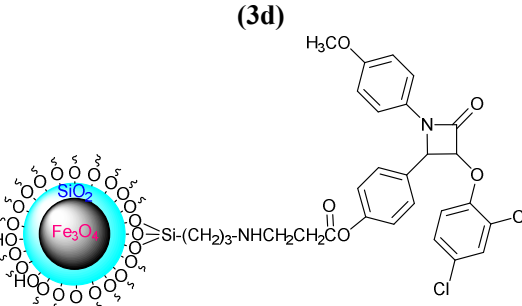
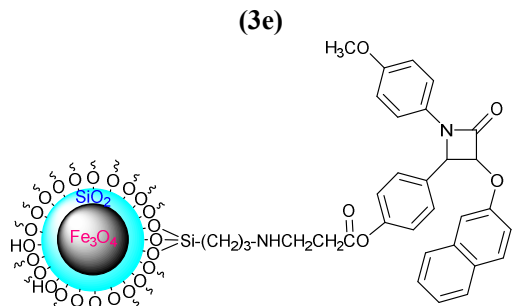
Finally, to synthesize β -lactam functionalized $\text{Fe}_3\text{O}_4@\text{SiO}_2$ nanoparticles ($\text{Fe}_3\text{O}_4@\text{SiO}_2/\beta$ -lactam) (**3a-f**), $\text{Fe}_3\text{O}_4@\text{SiO}_2\text{-NH}_2$ (**1**) was added to the solution of acrylate- β -lactams in THF and resulting mixture was stirred at $50\text{ }^\circ\text{C}$ for 5 h. After that, the product was removed by an external magnetic field, washed with ethanol and dried at $70\text{ }^\circ\text{C}$.

Table 1 depicts the TGA results of $\text{Fe}_3\text{O}_4@\text{SiO}_2/\beta$ -lactam nanoparticles under a nitrogen atmosphere. Based on the weight loss analysis given in Table1, the percentages of organic compounds (β -lactam) in $\text{Fe}_3\text{O}_4@\text{SiO}_2/\beta$ -lactam nanoparticles are 16.5-21.3 %.

N_2 adsorption-desorption isotherm analysis provide information on the specific surface area and porosity of the prepared samples. Adsorption-desorption isotherm measurements were conducted with N_2 for the $\text{Fe}_3\text{O}_4@\text{SiO}_2/\beta$ -lactam nanoparticles and result shown in Table1. BET surface area measurements have revealed that all samples present the adsorption isotherms characteristic of nanoparticles and show a similar surface area of ca. $410\text{-}430\text{ m}^2\text{g}^{-1}$.

Table 1. Structures of β -lactams (**2a-f**), $\text{Fe}_3\text{O}_4@\text{SiO}_2/\beta$ -lactams (**3a-f**) and their properties.

Entry	β -lactam	$\text{Fe}_3\text{O}_4@\text{SiO}_2/\beta$ -lactam	Properties	
			Functionalization (%) ^a	Surface area (m^2g^{-1}) ^b
1	(2a)	 (3a)	21.3 ± 0.02	415.2

2	(2b)		17.3 ± 0.04	424.0
3	(2c)		18.8 ± 0.05	416.5
4	(2d)		16.5 ± 0.02	417.1
5	(2e)		18.1 ± 0.03	410.5
6	(2f)		19.2 ± 0.04	428.0
		(3f)		

^aFunctionalized percentages were evaluated using thermogravimetric analysis.

^bSurface areas were evaluated from the N₂ adsorption isotherm.

The binding of β -lactam on surfaces of $\text{Fe}_3\text{O}_4@\text{SiO}_2$ nanoparticles was confirmed by FT-IR spectroscopy. Fig. 1 shows the FT-IR spectra of Fe_3O_4 , $\text{Fe}_3\text{O}_4@\text{SiO}_2$, $\text{Fe}_3\text{O}_4@\text{SiO}_2\text{-NH}_2$, β -lactam compounds and $\text{Fe}_3\text{O}_4@\text{SiO}_2/\beta$ -lactam in the 500-4000 cm^{-1} wave number range.

For pure magnetic nanoparticles exhibit a strong band at 570 cm^{-1} , characteristic of the Fe-O vibration correlated to the magnetic core and the peaks at around 3400 cm^{-1} and 1621 cm^{-1} are due to the O-H stretching and deforming vibrations of adsorbed water in the sample (Fig.1a).^{69,70} For all samples, the absorption peak at 570-580 cm^{-1} is observed, corresponding to the Fe-O vibration from the magnetite phase. The surfaces of pure Fe_3O_4 nanoparticles were readily covered with SiO_2 layers. The adsorption peaks at 1100 and 780 cm^{-1} corresponds to the antisymmetric and symmetric stretching vibration of Si-O-Si bond in oxygen-silica tetrahedron, respectively.⁷¹ In Fig. 1b, the unfunctionalized silica coated magnetite nanoparticles show stretches at 569, 1000-1150 and 3300 cm^{-1} , which can be attributed to the Fe-O, Si-O-Si, and -OH bonds, respectively. Fig.1c shows the FT-IR spectrum of $\text{Fe}_3\text{O}_4@\text{SiO}_2\text{-NH}_2$ nanoparticles, the peaks at 570, 1000-1150, 1400-1420 and 1561 cm^{-1} are attributed to Fe-O (stretching vibration), Si-O-Si (asymmetric stretching), C-N (stretching vibration) and N-H (bending), respectively. Also, the presence of several bands with medium intensity in 28010-2986 cm^{-1} and 3050-3250 regions are allocated to C-H stretching of propyl group and N-H stretching (Fig.1c).

Fig.1d-i shows the FT-IR spectrum of β -lactam compounds, the presence of absorbencies at 2860-3087, 1749-1762, 1670-1690, 1600-1630, 1480-1600, 1380-1390, 1200-1310, 1100-1200 are attributed to CH (stretching), C=O (amide stretching), C=O (ester stretching), C=C (acrylate stretching), C=C (aromatic ring stretching), CH_3 (bending), C-O (stretching) and C-N (stretching), respectively. From the IR spectra presented in Fig.1j-o, the absorption peaks at 570-580 cm^{-1} belonged to the stretching vibration mode of Fe-O bonds in Fe_3O_4 , the absorption peak presented at 1000-1150 cm^{-1} due to stretching vibration of framework and terminal Si-O-groups. The presence of vibration bands in 3400 (O-H stretching), 2850-3090 (C-H stretching), 1680-1750 (C=O amid and ketone stretching), 1560-1570 cm^{-1} (N-H bending), 1480-1600 (C=C aromatic ring stretching) and 1380-1390 (CH_3 bending) demonstrates the existence of β -lactam supported on $\text{Fe}_3\text{O}_4@\text{SiO}_2$ nanoparticles in the spectrum (Fig.1j-o).

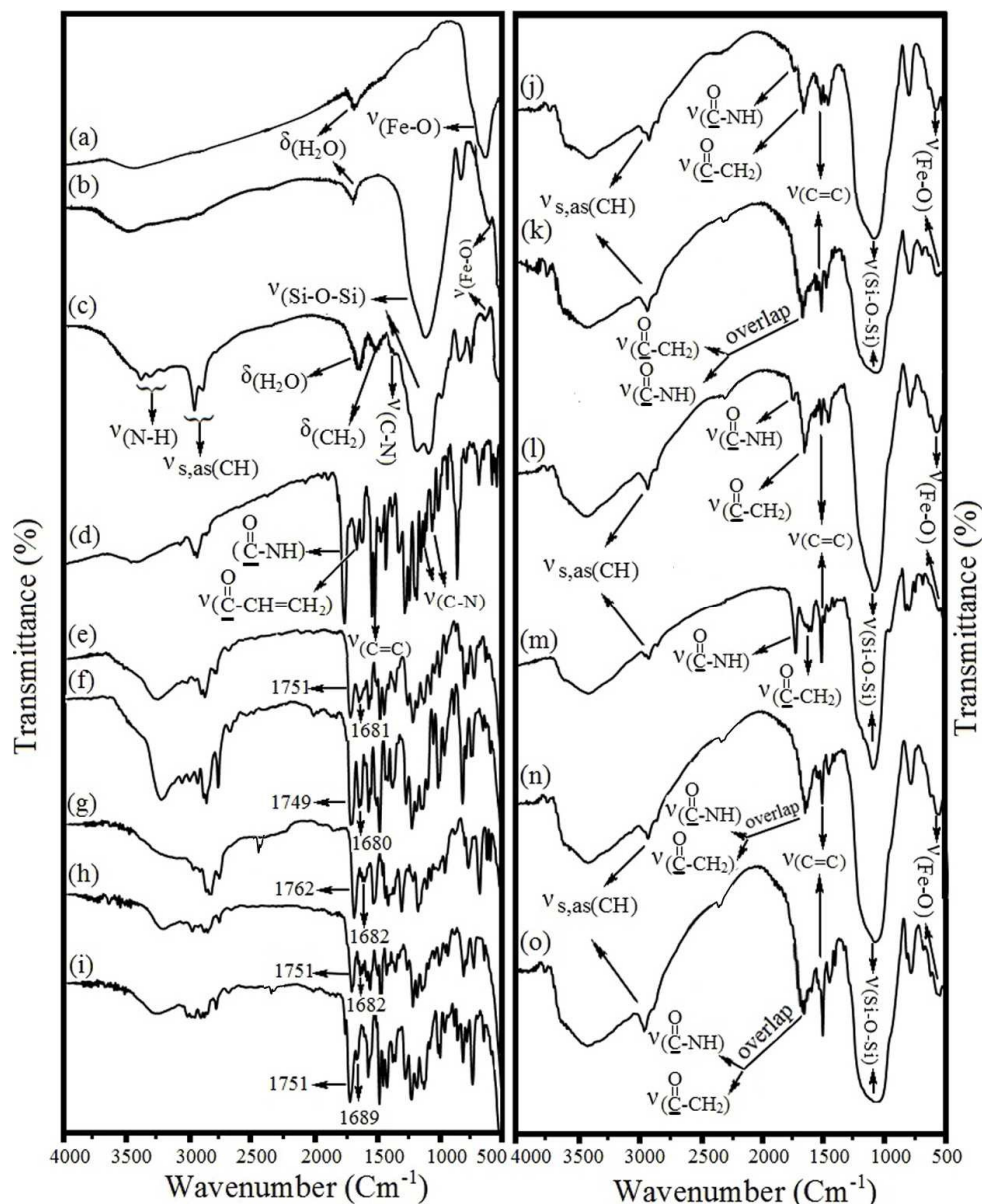


Fig 1. FT-IR spectra of Fe_3O_4 (a), $\text{Fe}_3\text{O}_4@SiO_2$ (b), $\text{Fe}_3\text{O}_4@SiO_2-NH_2$ (c), β -lactam (**2d**) (d), β -lactam (**2e**) (e), β -lactam (**2b**) (f), β -lactam (**2c**) (g), β -lactam (**2f**) (h), β -lactam (**2a**) (i), $\text{Fe}_3\text{O}_4@SiO_2/\beta$ -lactam (**3d**) (j), $\text{Fe}_3\text{O}_4@SiO_2/\beta$ -lactam (**3e**) (k), $\text{Fe}_3\text{O}_4@SiO_2/\beta$ -lactam (**3b**) (l), $\text{Fe}_3\text{O}_4@SiO_2/\beta$ -lactam (**3c**) (m), $\text{Fe}_3\text{O}_4@SiO_2/\beta$ -lactam (**3f**) (n) and $\text{Fe}_3\text{O}_4@SiO_2/\beta$ -lactam (**3a**) (o).

The crystalline structures of Fe_3O_4 , $\text{Fe}_3\text{O}_4@SiO_2$ and β -lactam supported on superparamagnetic $\text{Fe}_3\text{O}_4@SiO_2$ nanoparticles (**3a**) were studied by X-ray diffraction (XRD) analysis (Fig.2). The position and relative intensities of all peaks confirm well with standard XRD pattern of Fe_3O_4 (JCPDS card No. 85-1436) indicating retention of the crystalline cubic spinel structure during functionalization of MNPs.⁶⁴ The characteristic peaks at $2\theta = 30.1^\circ$, 35.4° , 43.1° , 53.4° , 57° and 62.6° for pure Fe_3O_4 nanoparticles, which were marked respectively by their indices (220), (311), (400),

(422), (511), and (440), were also observed for $\text{Fe}_3\text{O}_4@\text{SiO}_2$ and $\text{Fe}_3\text{O}_4@\text{SiO}_2/\beta$ -lactam (**3a**) nanoparticles (reference JCPDS card no.19-629).^{72,73} This revealed that modification on the surface of Fe_3O_4 nanoparticles did not lead to their phase change.

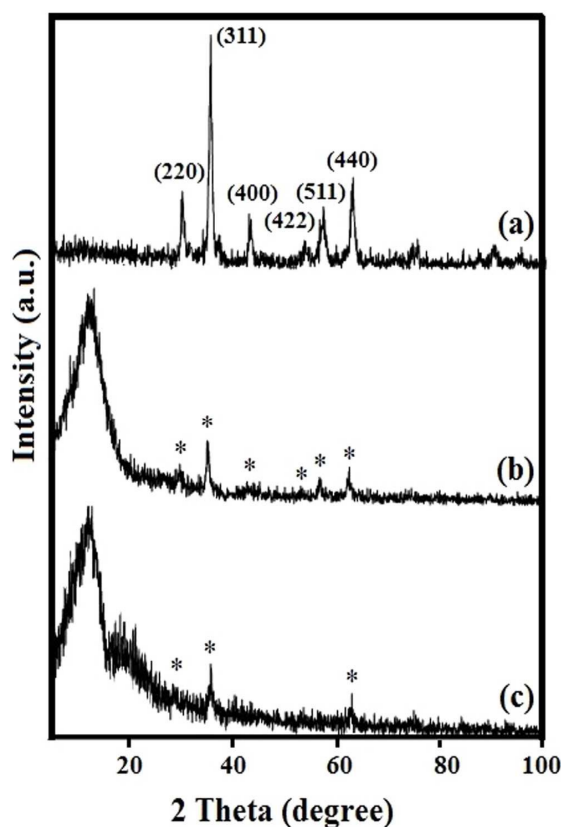


Fig 2. XRD patterns of Fe_3O_4 (a), $\text{Fe}_3\text{O}_4@\text{SiO}_2$ (b) and $\text{Fe}_3\text{O}_4@\text{SiO}_2/\beta$ -lactam (**3a**) (c).

The XRD pattern of $\text{Fe}_3\text{O}_4@\text{SiO}_2$ nanoparticles presented a broad featureless XRD peak at low diffraction angle ($2\theta=15\text{--}25^\circ$), which corresponded to the amorphous state SiO_2 shells (Fig.2b). For $\text{Fe}_3\text{O}_4@\text{SiO}_2/\beta$ -lactam (**3a**) nanoparticles, the broad peak was transferred to lower angles due to the synergetic effect of amorphous silica and β -lactam (Fig.2c). The mean size of the crystallites was calculated by applying Scherrer's equation: $D = 0.9\lambda/\beta \cos\theta$, where D is the average diameter in \AA , λ is the wavelength of the X-rays, β is the broadening of the diffraction line measured at half of its maximum intensity in radians and θ is the Bragg diffraction angle. The peak at $2\theta = 35.4^\circ$ is chosen to calculate the crystallite size, according to the result calculated by Scherrer equation, it is found that the diameter of Fe_3O_4 nanoparticles obtained is about 12 nm.

Transmission electron microscopy (TEM) was employed to characterize the morphology and size of Fe_3O_4 and $\text{Fe}_3\text{O}_4@\text{SiO}_2$. Fig.3a showed that the Fe_3O_4 nanoparticles had uniform spherical morphology with a uniform size of about 12 nm, corresponding with the result calculated by Scherrer equation.⁶⁴ After treatment by the modified Stober's reaction, the Fe_3O_4 particles were completely covered with a uniform transparent silica layer.

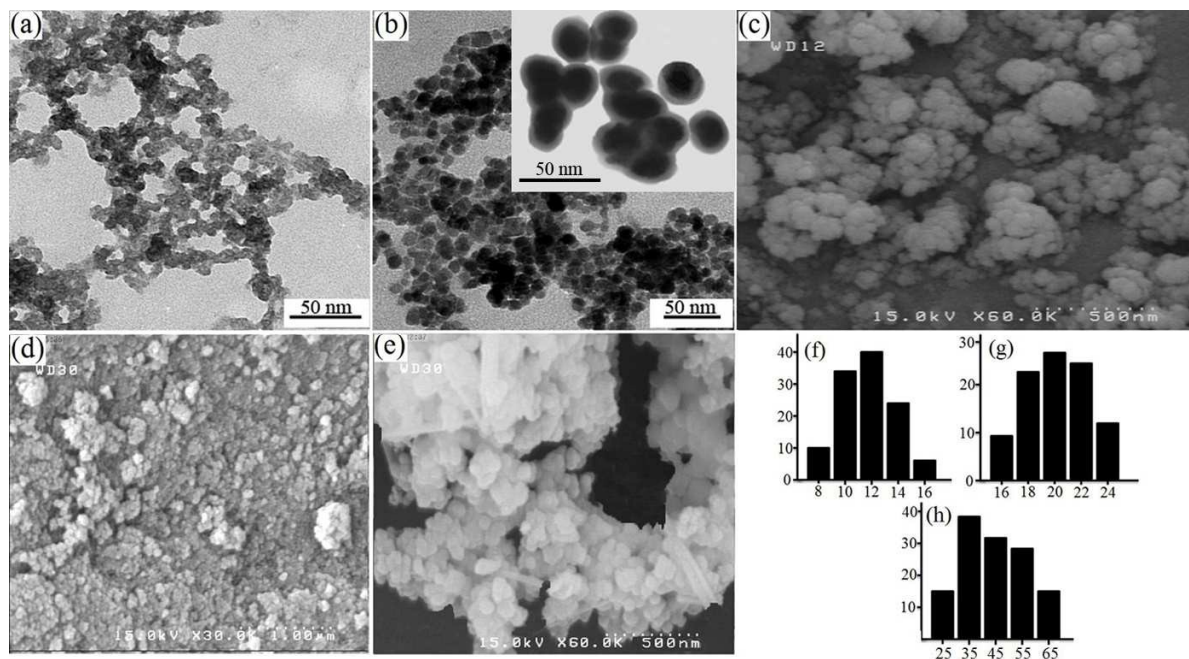


Fig 3. TEM images of a) Fe₃O₄, b) Fe₃O₄@SiO₂ and FE-SEM images of c) Fe₃O₄@SiO₂/β-lactam (**3a**), d) Fe₃O₄, e) Fe₃O₄@SiO₂ and the size distributions of f) Fe₃O₄, g) Fe₃O₄@SiO₂ and h) Fe₃O₄@SiO₂/β-lactam, respectively.

Furthermore, the particle size is roughly increased to 20 nm. The mesoporous silica shell on the surface of Fe₃O₄ is quite homogeneous and exhibits good monodispersity with estimated thickness of 8 nm.⁶⁴

The morphology and size of Fe₃O₄, Fe₃O₄@SiO₂ and Fe₃O₄@SiO₂/β-lactam (**3a**) nanoparticles were also observed by FE-SEM (Fig. 3). Uniform nanospheres of Fe₃O₄ with a diameter of approximately 15 nm were observed in Fig. 3d. The FE-SEM images indicate agglomerations of particles with homogenous size and the successful coating of the magnetic Fe₃O₄ particles (Fig. 3c,e). Fig. 3b and c shows that the Fe₃O₄@SiO₂ and Fe₃O₄@SiO₂/β-lactam (**3a**) nanoparticles are semispherical with an average size of 15-25 and 40-50 nm, respectively.

The hydrodynamic diameter of the Fe₃O₄, Fe₃O₄@SiO₂ and Fe₃O₄@SiO₂/β-lactam (**3a**) nanoparticles is determined by DLS technique. This size distribution is centered at a value of 12, 20 and 35 nm for Fe₃O₄, Fe₃O₄@SiO₂ and Fe₃O₄@SiO₂/β-lactam (**3a**), respectively (Fig 3f to h).

Fig. 4A depicts the TGA results of Fe₃O₄@SiO₂ and Fe₃O₄@SiO₂/β-lactam (**3a**) under a nitrogen atmosphere. The samples were measured in the condition of nitrogen atmosphere at the heating rate of 20°C/min until the temperature elevated to 650 °C. In the case of Fe₃O₄@SiO₂ nanoparticles the weight loss between 50 and 150 °C is due to loss of physically adsorbed water molecules (Fig.4Aa). Meanwhile, the weight loss above 200 °C was also possibly caused by the loss of structural water within amorphous SiO₂.⁷⁴

In this way, the slow slope appeared at the temperature range of 200-650 °C in the TGA curve of $\text{Fe}_3\text{O}_4@\text{SiO}_2$ (Fig.4Aa) can be explained. $\text{Fe}_3\text{O}_4@\text{SiO}_2/\beta$ -lactam shows two-step weight loss behavior (Fig.4.Ab). The initial weight loss 3.1 % from the $\text{Fe}_3\text{O}_4@\text{SiO}_2/\beta$ -lactam up to 130 °C is due to the removal of physically adsorbed solvent and surface hydroxyl groups. The two stages can be ascribed to the decomposition of β -lactam and organic volatile compounds. For $\text{Fe}_3\text{O}_4@\text{SiO}_2/\beta$ -lactam (**3a**), the mass loss of about 18.2 % by weight in the range of 150-450 °C is attributed to the decomposition of β -lactam (**2a**) and the temperature of the maximum weight loss is 420 °C.

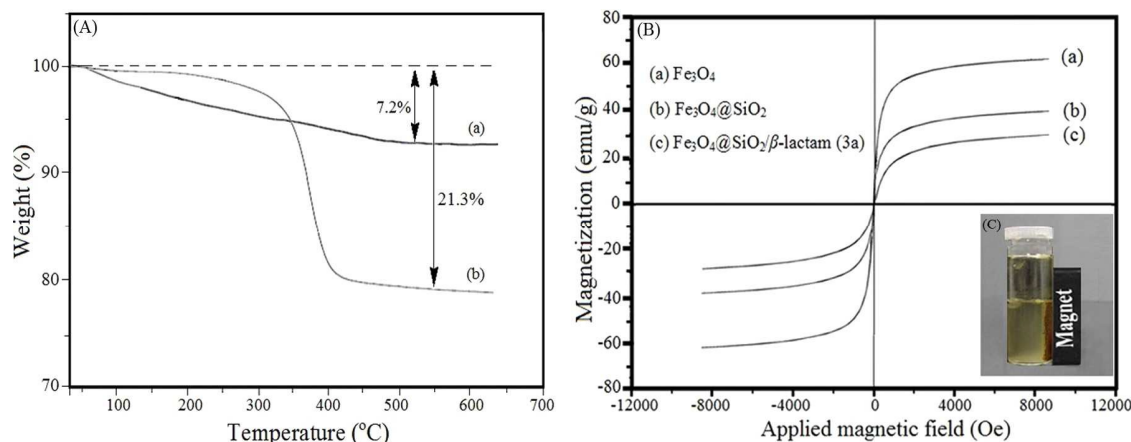


Fig 4. A) Thermogravimetric analysis of $\text{Fe}_3\text{O}_4@\text{SiO}_2$ (a) and $\text{Fe}_3\text{O}_4@\text{SiO}_2/\beta$ -lactam (**3a**) nanoparticles (b); B) Magnetization curves at 300 °K for Fe_3O_4 (a), $\text{Fe}_3\text{O}_4@\text{SiO}_2$ (b) and $\text{Fe}_3\text{O}_4@\text{SiO}_2/\beta$ -lactam (**3a**) nanoparticles (c); C) Magnetic separation image of $\text{Fe}_3\text{O}_4@\text{SiO}_2/\beta$ -lactam by an external magnet.

The magnetic property of the obtained samples was investigated using a vibrating sample magnetometer. The magnetic hysteresis loop of the magnetic nanoparticles Fe_3O_4 , $\text{Fe}_3\text{O}_4@\text{SiO}_2$ and $\text{Fe}_3\text{O}_4@\text{SiO}_2/\beta$ -lactam (**3a**) measured at $T = 300$ °K is shown in Fig. 4Ba,b,c and indicate that the magnetization saturation values of Fe_3O_4 , $\text{Fe}_3\text{O}_4@\text{SiO}_2$ and $\text{Fe}_3\text{O}_4@\text{SiO}_2/\beta$ -lactam (**3a**) are 62.4, 39.2 and 30.7 emu/g, respectively. It indicated that all products had superparamagnetism. No hysteresis curve was observed at the low magnetic field in the case of nanoparticles, and it was completely reversible at 300 °K. The magnetic reduction of the functionalized Fe_3O_4 nanoparticles was mostly attributed to the coating layer of the silica and β -lactam on the surface of Fe_3O_4 nanoparticles. Nevertheless, the β -lactam supported on superparamagnetic $\text{Fe}_3\text{O}_4@\text{SiO}_2$ can still be separated from the solution by using an external magnetic field on the sidewall of the reactor. As shown in Fig.4C inset, the magnetic separation was quickly fulfilled by supplying an external magnetic field near the suspension system of $\text{Fe}_3\text{O}_4@\text{SiO}_2/\beta$ -lactam.

2.2. Antibacterial activities

The antibacterial activity of β -lactam (**2a-f**) and β -lactam supported on $\text{Fe}_3\text{O}_4@\text{SiO}_2$ nanoparticles (**3a-f**) against gram-positive *S. aureus* (ATCC 25923) and gram-

negative *Escherichia coli* (ATCC 25922) bacterial strain were tested according reported method.⁷⁵ The minimum inhibitory concentrations (MICs) were defined as the lowest concentrations of the β -lactams (**2a-f**) and β -lactam supported on Fe₃O₄@SiO₂ nanoparticles (**3a-f**) that prevented visible growth and results were shown in Table 2. Also, standard antibacterial Fe₃O₄@SiO₂ nanoparticles were tested under the similar conditions for comparison. The results showed that Fe₃O₄@SiO₂ nanoparticles have no antibacterial activity against *E. coli*. The significant decrease of the MIC value for Fe₃O₄@SiO₂/ β -lactams suggests that the magnetic nanoparticles have improved the antibacterial activity of prepared β -lactams. The antibacterial activity of the functionalized Fe₃O₄@SiO₂ is related to the increasing of reactive oxygen species (ROS) which could damage the DNA of the bacterial cells and inhibit particular enzyme activities that are vital for cell growth without harming the human cells.^{76,77} These results indicated when β -lactams were connected covalently to Fe₃O₄@SiO₂ magnetic nanoparticles, a synergic effect was observed and the antibacterial inhibition of β -lactams were improved and among the Fe₃O₄@SiO₂/ β -lactams, those with the aryl substitution with chlorine atom on C-3 of β -lactam ring enhance the antibacterial activity.

Table 2. Antimicrobial activity of the β -lactams (**2a-f**) and Fe₃O₄@SiO₂/ β -lactams (**3a-f**) (MIC, $\mu\text{g}/\text{mL}$).

Compound	<i>S. aureus</i>	<i>E. coli</i>	Compound	<i>S. aureus</i>	<i>E. coli</i>
2a	50	100	3a	25	50
2b	25	100	3b	12.5	100
2c	25	100	3c	12.5	50
2d	50	100	3d	50	25
2e	50	50	3e	12.5	12.5
2f	50	100	3f	25	50
Fe₃O₄@SiO₂	100	na ^a			

^ana= no activity.

3. Conclusions

In summary, we have successfully prepared several novel β -lactam functionalized Fe₃O₄@SiO₂ nanoparticles for the first time. The FT-IR and TGA results demonstrated the formation β -lactams supported on superparamagnetic Fe₃O₄@SiO₂ nanoparticles. Both TEM and FE-SEM indicated that the Fe₃O₄@SiO₂ nanoparticles have been well-coated with β -lactams. XRD showed the significant effects of the Fe₃O₄ NPs on the crystallization behavior of the Fe₃O₄@SiO₂/ β -lactams. The vibrating sample magnetometer test showed that the saturation magnetization of the Fe₃O₄@SiO₂/ β -lactam (**3a**) was 30.7 emu/g and the presence of an external magnetic field would facilitate the separation of the Fe₃O₄@SiO₂/ β -lactams from the reaction mixture. Also, the results of antimicrobial activity study signified that supporting of β -lactams on superparamagnetic Fe₃O₄@SiO₂ nanoparticles provide a synergic effect and improve their antibacterial inhibition.

4. Experimental

4.1. Material and methods

The reagents and solvents used in this work were obtained from Fluka or Merck and used without further purification. Fourier transform infrared spectroscopy (FT-IR) analysis of the samples was taken on a Shimadzu FT-IR 8300 spectrophotometer and the sample and KBr were pressed to form a tablet. NMR spectra were recorded on a Bruker avance DPX 250 MHz spectrometer in CDCl_3 or $\text{DMSO}-d_6$ using tetramethylsilane (TMS) as an internal reference. The phase formation and crystallographic state of magnetic nanoparticles were determined by Bruker AXS D8-advance X-ray diffractometer with $\text{Cu K}\alpha$ radiation ($\lambda=1.5418$). The size and morphology of the nanoparticles were observed using a Philips EM208 transmission electron microscope (TEM) with an acceleration voltage 100 kV. The nanoparticles were thoroughly dispersed in water by ultra-sonication and placing a drop of solution on the carbon coated copper grid. Field Emission Scanning Electron Microscopy (FE-SEM) images were obtained on HITACHI S-4160. The hydrodynamic size of the particle was measured by dynamic light scattering (DLS) techniques, using a HORIBA-LB550 particle size analyzer. The BET surface area and porosity of catalysts were determined from nitrogen physisorption measured on a Micromeritics ASAP 2000 instrument at -196 °C. Thermogravimetric analysis (TGA) was carried out using Perkin Elmer with N_2 carrier gas and the rate of temperature change of 20 °C min^{-1} . The magnetic properties of the composite nanoparticles were measured by BHV-55 vibrating sample magnetometer (VSM) 298 °K. Melting points were determined on a Mel-Temp apparatus and are Uncorrected. Elemental analysis was done on a 2400 series Perkin-Elmer analyzer. The mass spectra were recorded on a Shimadzu GC-MS QP 1000 EX instrument. Determination of the purity of the substrate and monitoring of the reaction were accomplished by thin-layer chromatography (TLC) and purification was achieved by silica gel column chromatography.

4.2. General procedure

2.2.1. Preparation of $\text{Fe}_3\text{O}_4@\text{SiO}_2$ core-shell

The core-shell $\text{Fe}_3\text{O}_4@\text{SiO}_2$ nanospheres were prepared by a modified Stober method in our previous work.^{78, 79}

4.2.2. Preparation of magnetic nanoparticles coated by (3-aminopropyl)-triethoxysilane ($\text{Fe}_3\text{O}_4@\text{SiO}_2\text{-NH}_2$)

The obtained $\text{Fe}_3\text{O}_4@\text{SiO}_2$ powder (1 g) was dispersed in 10 mL ethanol solution by sonication for 20 min, and then 3-aminopropyl (triethoxy) silane (2 mmol, 0.352 g)

was added to the mixture. After mechanical stirred under reflux conditions for 12 h, the suspended substance ($\text{Fe}_3\text{O}_4@\text{SiO}_2\text{-NH}_2$) was separated with the external magnetic field. Then, the product was washed with ethanol and water to remove no reacted species and dried at 80 °C for 6 h.

4.2.3. General procedure for the preparation of Schiff base 4-(((4-methoxy phenyl) imino) methyl) phenol (**1a**)

A mixture of 4-methoxyaniline (1 mmol) and 4-hydroxybenzaldehyde (1 mmol) was refluxed in ethanol (20 mL) for 5 hours. After cooling, the resulting Schiff base, as the gray precipitate, was separated by filtration and washed with ethanol (5 mL) and then dried in vacuum. The crude product was recrystallized from ethanol to obtain the pure product in 88 % yield.

4.2.4. General procedure for the preparation of 4-(((4-methoxyphenyl) imino) methyl) phenyl acrylate (**1b**)

To the solution of **1a** (1 mmol) in 10 mL of CH_2Cl_2 was added triethylamine (2.2 mmol). Acryloyl chloride (2.2 mmol) was added dropwise to the solution at 0 °C. The resulting solution was stirred at room temperature for 15 minutes, and then washed with H_2O (2×10 mL). The organic layer was dried with anhydrous MgSO_4 , filtered, and evaporated. The crude of acrylate imine **1b**, as oil, was used for the next step.

4.2.5. General procedure for the preparation of acrylate- β -lactams (**2a-f**)

A mixture of crude Schiff base **1b**, triethylamine (5 mmol), 9H-xanthen-9-carboxylic acid or derivatives of oxyacetic acid (1.5 mmol) and tosyl chloride (1.5 mmol) in dry CH_2Cl_2 (15 mL) was stirred at room temperature for overnight. Then it was washed with HCl 1N (20 mL), saturated NaHCO_3 (20 mL) and brine (20 mL). The organic layer was dried over Na_2SO_4 , filtered and the solvent was evaporated to give the product as a solid which was then purified by column chromatography (EtOAc/Petroleum ether (8/2)).

4.2.6. General procedure for the preparation of β -lactam functionalized $\text{Fe}_3\text{O}_4@\text{SiO}_2$ nanoparticles ($\text{Fe}_3\text{O}_4@\text{SiO}_2/\beta$ -lactam) (**3a-f**)

$\text{Fe}_3\text{O}_4@\text{SiO}_2\text{-NH}_2$ (1 g) was added to the solution of acrylate- β -lactams (1 mmol) in THF (5 mL) and the resultant mixture was stirred at 50 °C for 5 h. The resulting solid was removed by an external magnetic field. Then the solid was washed with ethanol to eliminate any impurities in the solid and dried at 70 °C for 4 h. FT-IR (KBr pellets, cm^{-1}): $\text{Fe}_3\text{O}_4@\text{SiO}_2/\beta$ -lactam (**3a**): 3400 (O-H), 2846-3070 (C-H stretching), 1690-1750 (overlap $2\text{C}=\text{O}$ amide and ester, stretching), 1480-1600 (C=C aromatic ring), 1462 (CH_2 bending), 1396 (CH_3 bending), 1000-1150 (Si-O-Si asymmetric stretching), 571 (Fe-O stretching). $\text{Fe}_3\text{O}_4@\text{SiO}_2/\beta$ -lactam (**3b**): 3400 (O-H), 2854-3076 (C-H stretching), 1736 (C=O amide, stretching), 1691 (C=O ester, stretching),

1480-1600 (C=C aromatic ring), 1464 (CH₂ bending), 1374, 1395 (2CH₃ bending), 1000-1150 (Si-O-Si asymmetric stretching), 573 (Fe-O stretching). Fe₃O₄@SiO₂/β-lactam (**3c**): 3400 (O-H), 2854-3076 (C-H stretching), 1745 (C=O amide, stretching), 1694 (C=O ester, stretching), 1480-1600 (C=C aromatic ring), 1462 (CH₂ bending), 1373 (CH₃ bending), 1000-1150 (Si-O-Si asymmetric stretching), 570 (Fe-O stretching). Fe₃O₄@SiO₂/β-lactam (**3d**): 3400 (O-H), 2857-3069 (C-H stretching), 1748 (C=O amide, stretching), 1698 (C=O ester, stretching), 1480-1600 (C=C aromatic ring), 1476 (CH₂ bending), 1369 (CH₃ bending), 1000-1150 (Si-O-Si asymmetric stretching), 571 (Fe-O stretching). Fe₃O₄@SiO₂/β-lactam (**3e**): 3400 (O-H), 2862-3085 (C-H stretching), 1690-1750 (overlap 2C=O amide and ester, stretching), 1480-1600 (C=C aromatic ring), 1472 (CH₂ bending), 1392 (CH₃ bending), 1000-1150 (Si-O-Si asymmetric stretching), 570 (Fe-O stretching). Fe₃O₄@SiO₂/β-lactam (**3f**): 3400 (O-H), 2870-3072 (C-H stretching), 1690-1750 (overlap 2C=O amide and ester, stretching), 1480-1600 (C=C aromatic ring), 1458 (CH₂ bending), 1388 (CH₃ bending), 1000-1150 (Si-O-Si asymmetric stretching), 570 (Fe-O stretching).

4.2.7. Determination of minimum inhibitory concentrations (MICs)

Gram-positive *S. aureus* (ATCC 25923) and gram-negative *Escherichia coli* (ATCC 25922) bacterial strain were used as test bacteria. Cultures were grown in 10 mL of Brain Heart Infusion solution and incubated for overnight at 37 °C and shaking at 100 rpm. These cultures were washed and diluted to a final concentration of 5×10^5 bacteria/mL in Brain Heart Infusion solution containing various concentrations of free of β-lactam (**2a-f**) or Fe₃O₄@SiO₂/β-lactam (**3a-f**) (ranging from 0 to 100 μg/mL). Bacterial densities were estimated by diluting method after incubation at 37 °C and shaking at 200 rpm for 24 h, then plating bacterial on Brain Heart Infusion agar followed by incubation overnight at 37 °C. The MIC was determinate as the last dilution of the tested samples which inhibited the microbial growth.

Spectral data

Schiff base 4-(((4-methoxyphenyl)imino)methyl)phenol (**1a**)

Gray solid, mp 200-203 °C; ¹H NMR (250 MHz, DMSO-*d*₆): δ = 3.79 (s, 3H, OMe), 6.85-6.91 (m, 4H, Ar-H), 7.17 (d, *J* = 8.00 Hz, 2H, Ar-H), 7.72 (d, *J* = 8.00 Hz, 2H, Ar-H), 8.38 (s, 1H, CH=N), 9.75 (s, 1H, OH); ¹³C NMR (62.9 MHz, DMSO-*d*₆): δ = 60.2 (OMe), 119.1, 120.5, 126.8, 132.7, 135.1, 149.9, 160.0, 162.6, 165.3 (C=N); IR (Neat, Cm⁻¹): 1027, 1243 (sp²C-O-Csp³), 1390 (CH₃ bending), 1480-1600 (C=C aromatic ring), 1638 (C=N stretching), 2844-3075 (CH stretching); Analysis calculated for C₁₄H₁₃NO₂: C, 73.99; H, 5.77; N, 6.16%. Found: C, 73.71; H, 5.51; N, 5.65%.

4-(1-(4-Methoxyphenyl)-2-oxospiro[azetidine-3,9'-xanthen]-4-yl)phenyl acrylate (**2a**)

Yellow oil, ¹H NMR (250 MHz, CDCl₃): δ = 3.80 (s, 3H, OMe), 5.08 (d, *J* = 4.75 Hz, 1H, H-3), 5.93-5.98 (m, 1H, acrylat), 6.21-6.25 (m, 1H, acrylat), 6.49-6.52 (m, 1H, acrylat), 6.84-7.50 (m, 16H, Ar-H); ¹³C NMR (62.9 MHz, CDCl₃): δ = 55.5 (OMe), 63.9 (C-4), 73.8 (C-3),

114.5, 116.2, 116.9, 119.0, 121.3, 122.7, 124.3, 127.6, 128.4, 129.1, 131.3, 132.2, 132.8, 149.9, 152.0, 156.6, 164.2 (CO acrylat), 165.6 (CO β -lactam). MS m/z = 489 [M^+]. IR (Neat, cm^{-1}): 1384 (CH_3 bending), 1480-1600 (C=C aromatic ring), 1607 ($-\text{CH}=\text{CH}_2$ acrylat), 1689 (C=O acrylat), 1751 (C=O β -lactam), 2839-3082 (CH stretching). Analysis calculated for $\text{C}_{31}\text{H}_{23}\text{NO}_5$: C, 76.06; H, 4.74; N, 2.86%. Found: C, 76.51; H, 4.93; N, 2.93%.

4-(3-Methoxy-1-(4-methoxyphenyl)-4-oxoazetidin-2-yl) phenyl acrylate (2b)

Yellow oil, ^1H NMR (250 MHz, CDCl_3): δ = 3.73 (s, 3H, OMe), 3.77 (s, 3H, OMe), 4.80 (d, J = 4.70 Hz, 1H, H-4), 5.19 (d, J = 4.70 Hz, 1H, H-3), 5.69-5.73 (m, 1H, acrylat), 6.00-6.05 (m, 1H, acrylat), 6.56-6.64 (m, 1H, acrylat), 6.76-7.51 (m, 8H, Ar-H); ^{13}C NMR (62.9 MHz, CDCl_3): δ = 55.4, 58.4 (OMe), 61.3 (C-4), 84.7 (C-3), 114.1, 114.4, 116.1, 118.8, 122.0, 127.4, 129.0, 131.1, 132.3, 132.9, 156.4, 163.0 (CO acrylat), 163.8 (CO β -lactam); MS m/z = 353.2 [M^+]; IR (Neat, Cm^{-1}): 1387 (CH_3 bending), 1480-1600 (C=C aromatic ring), 1608 ($-\text{CH}=\text{CH}_2$ acrylat), 1680 (C=O acrylat), 1749 (C=O β -lactam), 2839-3071 (CH stretching); Analysis calculated for $\text{C}_{20}\text{H}_{19}\text{NO}_5$: C, 67.98; H, 5.42; N, 3.96%. Found: C, 68.21; H, 5.53; N, 4.03%.

4-(1-(4-Methoxyphenyl)-4-oxo-3-phenoxyazetidin-2-yl) phenyl acrylate (2c)

White solid, mp 155-157 $^\circ\text{C}$; ^1H NMR (250 MHz, CDCl_3): δ = 3.74 (s, 3H, OMe), 5.36 (d, J = 4.70 Hz, 1H, H-4), 5.55 (d, J = 4.70 Hz, 1H, H-3), 5.96-6.01 (m, 1H, acrylat), 6.21-6.32 (m, 1H, acrylat), 6.53-6.60 (m, 1H, acrylat), 6.79-7.39 (m, 13H, Ar-H); ^{13}C NMR (63 MHz, CDCl_3): δ = 55.4 (OMe), 61.4 (C-4), 81.1 (C-3), 114.4, 115.7, 118.9, 121.5, 122.2, 127.7, 129.1, 129.3, 129.5, 130.2, 132.7, 150.8, 156.5, 156.8, 162.3 (CO acrylat), 164.1 (CO β -lactam); MS m/z = 415.1 [M^+]; IR (Neat, Cm^{-1}): 1381 (CH_3 bending), 1480-1600 (C=C aromatic ring), 1612 ($-\text{CH}=\text{CH}_2$ acrylat), 1682 (C=O acrylat), 1762 (C=O β -lactam), 2843-3078 (CH stretching); Analysis calculated for $\text{C}_{25}\text{H}_{21}\text{NO}_5$: C, 72.28; H, 5.10; N, 3.37; %. Found: C, 71.98; H, 4.03; N, 3.21; %.

4-(3-(4-Chlorophenoxy)-1-(4-methoxyphenyl)-4-oxoazetidin-2-yl)phenyl acrylate (2d)

Light yellow oil, ^1H NMR (250 MHz, CDCl_3): δ = 3.74 (s, 3H, OMe), 5.36 (d, J = 4.75 Hz, 1H, H-4), 5.50 (d, J = 4.75 Hz, 1H, H-3), 6.02-6.03 (m, 1H, acrylat), 6.23-6.34 (m, 1H, acrylat), 6.55-6.62 (m, 1H, acrylat), 6.70-6.82 (m, 4H, Ar-H), 7.08-7.14 (m, 4H, Ar-H), 7.26-7.39 (m, 4H, Ar-H); ^{13}C NMR (62.9 MHz, CDCl_3): δ = 55.4 (OMe), 61.3 (C-4), 81.3 (C-3), 114.4, 115.9, 117.0, 118.9, 121.6, 127.7, 129.1, 129.2, 129.4, 130.0, 132.9, 150.9, 155.4, 156.6, 162.0 (CO acrylat), 164.2 (CO β -lactam); MS m/z = 449 [M^+]; IR (Neat, Cm^{-1}): 1393 (CH_3 bending), 1480-1600 (C=C aromatic ring), 1628 ($-\text{CH}=\text{CH}_2$ acrylat), 1681 (C=O acrylat), 1736 (C=O β -lactam), 2869-3078 (CH stretching); Analysis calculated for $\text{C}_{25}\text{H}_{20}\text{ClNO}_5$: C, 66.74; H, 4.48; N, 3.11%. Found: C, 66.25; H, 4.39; N, 3.08%.

4-(3-(2,4-Dichlorophenoxy)-1-(4-methoxyphenyl)-4-oxoazetidin-2-yl)phenyl acrylate (2e)

Light yellow oil, ^1H NMR (250 MHz, CDCl_3): δ = 3.74 (s, 3H, OMe), 5.40 (d, J = 4.70 Hz, 1H, H-4), 5.50 (d, J = 4.70 Hz, 1H, H-3), 5.98-6.18 (m, 1H, acrylat), 6.30-6.35 (m, 1H, acrylat), 6.55-6.62 (m, 1H, acrylat), 6.92-7.34 (m, 11H, Ar-H); ^{13}C NMR (62.9 MHz, CDCl_3): δ = 55.4 (OMe), 60.9 (C-4), 81.6 (C-3), 114.5, 116.0, 118.9, 121.7, 122.3, 124.2, 127.4, 127.7, 129.1, 130.0, 131.2, 132.3, 132.9, 151.0, 151.4, 156.7, 161.7 (CO acrylat), 162.7 (CO β -lactam); MS m/z = 483.3 [M^+]; IR (Neat, Cm^{-1}): 1389 (CH_3 bending), 1480-1600 (C=C aromatic ring), 1612 ($-\text{CH}=\text{CH}_2$ acrylat), 1681 (C=O acrylat), 1751 (C=O β -lactam), 2885-3086 (CH stretching); Analysis calculated for $\text{C}_{25}\text{H}_{19}\text{Cl}_2\text{NO}_5$: C, 62.00; H, 3.95; N, 2.89%. Found: C, 62.11; H, 4.02; N, 2.95%.

4-(1-(4-Methoxyphenyl)-3-(naphthalen-2-yloxy)-4-oxoazetidin-2-yl)phenyl acrylate (2f)

Brown oil, ^1H NMR (250 MHz, CDCl_3): δ = 3.72 (s, 3H, OMe), 5.39 (d, J = 4.65 Hz, 1H, H-4), 5.65 (d, J = 4.70 Hz, 1H, H-3), 5.94-5.98 (m, 1H, acrylat), 6.23-6.33 (m, 1H, acrylat), 6.51-6.81 (m, 1H, acrylat), 6.90-7.75 (m, 15H, Ar-H); ^{13}C NMR (62.9 MHz, CDCl_3): δ = 55.4 (OMe), 61.5 (C-4), 81.0 (C-3), 109.2, 114.0, 114.4, 116.0, 118.3, 118.9, 121.5, 121.9, 124.2, 126.4, 126.8, 127.6, 129.1, 129.5, 130.1, 131.0, 132.2, 132.8, 133.8, 156.6, 162.4 (CO acrylat), 163.8 (CO β -lactam); MS m/z = 465 [M^+]; IR (Neat, Cm^{-1}): 1389 (CH_3 bending), 1480-1600 (C=C aromatic ring), 1605 (-CH=CH₂ acrylat), 1682 (C=O acrylat), 1751 (C=O β -lactam), 2831-3070 (CH stretching); Analysis calculated for $\text{C}_{29}\text{H}_{23}\text{NO}_5$: C, 74.83; H, 4.98; N, 3.01%. Found: C, 74.97; H, 5.11; N, 3.13%.

Acknowledgements

Authors are grateful to the research council of Shiraz University and Iran National Science Foundation for their financial support to undertake this work.

References

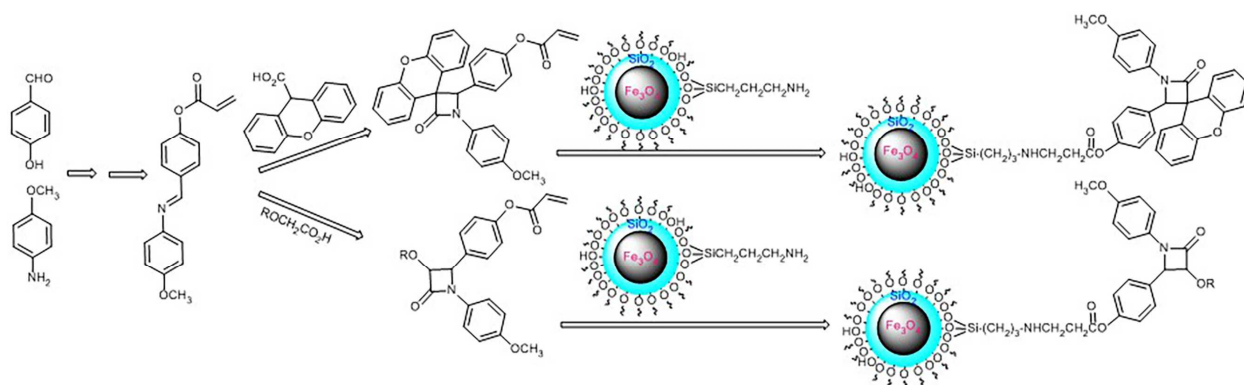
- 1 K.A. Jolliffe, *Inhibitors of fungal phospholipase B: novel antifungal agents. Congdes of drug design*. Amongst The Vines, Hunter Valley, NSW, Australia, 2006.
- 2 A. Jarrahpour, J. Sheikh, I. El Mounsi, H. Juneja and T.B. Hadda, *Med. Chem. Res.*, 2013, **22**, 1203-1211.
- 3 A. Fernandez-Gonzalez, R. Badia and M.E. Diaz-Garcia, *Anal. Biochem.*, 2005, **341**, 113-121.
- 4 R. Southgate, *Contemp. Org.Synth.*, 1994, **1**, 417-431.
- 5 T.E. Long and E. Turos, *Curr. Med. Chem. Anti-Infect. Agents.*, 2002, **1**, 251-268.
- 6 B. Alcaide, P. Almendros, G. Cabrero and M.P. Ruiza, *Synthesis.*, 2008, **17**, 2835-2839.
- 7 E. Leemans, M. D'hooghe, Y. Dejaegher, K.W. Tornroos and N. De Kimpe, *J. Org.Chem.*, 2008, **73**, 1422-1428.
- 8 R.K. Mishra, C.M. Coates, K.D. Revell and E. Turos, *Org. Lett.*, 2007, **9**, 575-578.
- 9 L.R. Domingo, M.J. Aurell and M. Arno, *Tetrahedron.*, 2009, **65**, 3432-3440.
- 10 A.K. Halve, D. Bhadauria and R. Dubey, *Bioorg. Med. Chem. Lett.*, 2007, **17**, 341-345.
- 11 A. Jarrahpour, E. Ebrahimi, R. Khalifeh, H. Sharghi, M. Sahraei, V. Sinou, C. Latour and J.M. Brunel, *Tetrahedron.*, 2012, **68**, 4740-4744.
- 12 T. Sperka, J. Pitlik, P. Bagossi and J. Tozser, *Bioorg. Med. Chem. Lett.*, 2005, **15**, 3086-3090.
- 13 A. Jarrahpour, E. Ebrahimi, E. De Clercq, V. Sinou, C. Latour, L. Djouhri Bouktab and J.M. Brunel, *Tetrahedron.*, 2011, **67**, 8699-8704.
- 14 G. Veinberg, I. Shestakova, M. Verma, I. Kenepe and E. Lukevics, *Bioorg. Med. Chem. Lett.*, 2004, **14**, 147-150.
- 15 R.K. Goel, M.P. Mahajan and S.K. Kulkarni, *J. Pharm. Pharm. Sci.*, 2004, **7**, 80-83.
- 16 C. Saturnino, B. Fusco, P. Saturnino, G. De Martino, F. Rocco and J.C. Lanceolat, *Biol. Pharm. Bull.*, 2000, **23**, 654-656.
- 17 S.B. Rosenblum, T. Huynh, A. Afonso, H.R. Davis, N. Yumibe, J.W. Clader and D.A. Burnett, *J. Med. Chem.*, 1998, **41**, 973-980.
- 18 W.T. Han, A.K. Trehan, J.J.K. Wright, M.E. Federici, S.M. Seiler and N.A. Meanwell, *Bioorg. Med. Chem.*, 1995, **3**, 1123-1143.
- 19 M.I. Konaklieva, *Curr. Med. Chem. Anti-Infective. Agents.*, 2002, **1**, 215-238.
- 20 A.D. Borthwick, G. Weingarte, T.M. Haley, M. Tomaszewski, W. Wang, Z. Hu, J. Bedard, H. Jin, L. Yuen and T.S. Mansour, *Bioorg. Med. Chem. Lett.*, 1998, **8**, 365-370.
- 21 J. Marchand-Brynaert, M. Laurent and M. Ceresiat, *J. Org. Chem.*, 2004, **69**, 3194-3197.
- 22 M.A. Bonache, G. Gerona-Navarro, C. Garcia-Aparicio, M. Alias, M. Martin-Martinez, M.T.

- Garcia- Lopez, P. Lopez, C. Cativiela and R. Gonzalez-Muniz, *Tetrahedron Asymmetry*, 2003, **14**, 2161-2169.
- 23 X. Zhang, R.P. Hsung, H. Li, Y. Zhang, W.L. Johnson and R. Figueroa, *Org. Lett.*, 2008, **10**, 3477-3479.
- 24 E. Bandini and G. Favi, *Org. Lett.*, 2000, **2**, 1077-1079.
- 25 S. Hata, T. Iwasawa, M. Iguchi, K. Yamada and K. Tomioka, *Synthesis*, 2004, **9**, 1471-1475.
- 26 H. Staudinger, *Liebigs Ann. Chem.*, 1907, **356**, 51-123.
- 27 F.H. Van der Steen and G. Van Koten, *Tetrahedron*, 1991, **47**, 7503-7524.
- 28 A. Jarrahpour and P. Alvand, *Iran. J. Sci. Tech. Trans. A.*, 2007, **31**, 17-22.
- 29 G.I. Georg, *The Organic Chemistry of β -Lactams*, VCH: New York, 1993.
- 30 A. Jarrahpour and M. Zarei, *Tetrahedron*, 2009, **65**, 2927-2934.
- 31 A.K. Bose, J.C. Kapur, S.D. Sharma and M.S. Manhas, *Tetrahedron Lett.*, 1973, **14**, 2319-2320.
- 32 A.R.A.S. Deshmukh, D. Krishnaswamy, V.V. Govande, B.M. Bhawal and V.K. Gumaste, *Tetrahedron*, 2002, **58**, 2215-2225.
- 33 M.S. Manhas, A.K. Bose and M.S. Khajavi, *Synthesis*, 1981, **46**, 209-210.
- 34 M. Nahmany and A. Melman, *J. Org. Chem.*, 2006, **71**, 5804-5806.
- 35 A. Bhalla, P. Venugopalany and S.S. Bari, *Tetrahedron*, 2006, **62**, 8291-8302.
- 36 P.D. Croce and C. La Rosa, *Tetrahedron Asymmetry*, 1999, **10**, 1193-1199.
- 37 S. Matsui, Y. Hashimoto and K. Saigo, *Synthesis*, 1998, **8**, 1161-1166.
- 38 E. Ebrahimi and A. Jarrahpour, *Iran. J. Sci. Technol. A.*, 2014, **38**, 49-53.
- 39 S. Shen, J.X. Xia and J. Wang, *Biomaterials*, 2016, **74**, 1-18.
- 40 P. Pengo and L. Pasquato, *J. Fluorine Chem.*, 2015, **117**, 2-10.
- 41 E. Reimhult, *New. Biotechnol.*, 2015, **32**, 665-672.
- 42 J.B. Blanco-Canosa, M. Wu, K. Susumu, E. Petryayeva, T.L. Jennings, P.E. Dawson, W.R. Algar, and I.L. Medintz, *Coordin. Chem. Rev.*, 2014, **263**, 101-137.
- 43 S.V. Salihov, Y.A. Ivanenkov, S.P. Krechetov, M.S. Veselov, N.V. Sviridenkova, A.G. Savchenko, N.L. Klyachko, Y.I. Golovin, N.V. Chufarova, E.K. Beloglazkina and A.G. Majouga, *J. Magn. Magn. Mater.*, 2015, **394**, 173-178.
- 44 E. Ebrahimi, A. Jarrahpour, N. Heidari, V. Sinou, C. Latour, J.M. Brunel, A.R. Zolghadr and E. Turos, *Med. Chem. Res.*, 2016, **25**, 247-262.
- 45 A. Jarrahpour, M.M. Doroodmand and E. Ebrahimi, *Tetrahedron Lett.*, 2012, **53**, 2797-2801.
- 46 I. Capek, *Adv. Colloid. Interface.*, 2015, **222**, 119-134.
- 47 A. Dehshahri and H. Sadehpour, *Colloid. Surface. B.*, 2015, **132**, 85-102.
- 48 P. Kesharwani, S. Banerjee, U. Gupta, M.C.I.M. Amin, S. Padhye, F.H. Sarkar and A.K. Iyer, *Mater. Today*, 2015, **18**, 565-572.
- 49 L. Douziech-Eryrolles, H. Marchais and K. Herve, *Int. J. Nanomedicine*, 2007, **2**, 541-550.
- 50 G. Reiss and A. Huetten, *Nat Mater.*, 2005, **4**, 725-726.
- 51 T. Hyeon, *Chem Commun.*, 2003, **8**, 927-934.
- 52 C.T. Yavuz, J.T. Mayo, W.W. Yu, A. Prakash, J.C. Falkner, S. Yean, L.L. Cong, H.J. Shipley, A. Kan, M. Tomson, D. Natelson and V.L. Colvin, *Science*, 2006, **314**, 964-967.
- 53 J.W.M. Bulte and D.L. Kraitman, *NMR Biomed.*, 2004, **17**, 484-499.
- 54 C. Corot, M. Port, I. Guilbert, P. Robert, I. Raynal, C. Robic, J.S. Raynaud, P. Prigent, A. Dencausse, J. Idee, *Superparamagnetic Contrast Agents*, In: M.M.J. Modo, W.M. Jeff, J.W.M. Bulte (Eds.), *Molecular and Cellular MR Imaging*, CRC Press, Boca Raton, FL, 2007, 60-78.
- 55 A.H. Lu, W. Schmidt, N. Matoussevitch, H. Bönemann, B. Spliethoff, B. Tesche, E. Bill, W.Kiefer and F. Schüth, *Angew. Chem.*, 2004, **116**, 4403-4406.
- 56 A. Ito, H. Honda and T. Kobayashi, *Cancer. Immunol. Immun.* 2006, **55**, 320-328.
- 57 B. Thiesen and A. Jordan, *Int. J. Hyperthermia*, 2008, **24**, 467-474.
- 58 J. Javidi and M. Esmaeilpour, *Colloid. Surface B.*, 2013, **102**, 265-272.
- 59 P. Xue, W.G. Su, Y.H. Gu, H.F. Liu and J.L. Wang, *J. Magn. Magn. Mater.*, 2015, **378**, 306-312.
- 60 P. Xue, Y. Gu, W. Su, H. Shuai and J. Wang, *Appl. Surf. Sci.*, 2016, **362**, 427-433.
- 61 U.A. Hasanova, M.A. Ramazanov, A. M. Maharramov, Q.M. Eyvazova, Z.A. Agamaliyev, Y.V. Parfyonova, S.F. Hajiyeva, F.V. Hajiyeva and S.B. Veliyeva, *J. Biomater. Nanobiotechnol.*, 2015, **6**, 225-235.

- 62 A.M. Grumezescu, M.C. Gestal, A.M. Holban, V. Grumezescu, B.S. Vasile, L. Mogoantă, F. Iordache, C. Bleotu and G.D. Mogoşanu, *Molecules.*, 2014, **19**, 5013-5027.
- 63 M. Esmailpour, J. Javidi, F. Nowroozi Dodeji and M. Mokhtari Abarghoui, *J. Mol. Catal. A: Chem.*, 2014, **393**, 18-29.
- 64 J. javidi, M. Esmailpour, F. Dehghani and F. Nowroozi Dodeji, *RSC Adv.*, 2015, **5**, 26625-26633.
- 65 J. Javidi and M. Esmailpour, *Mater. Res. Bull.*, 2016, **73**, 409-422.
- 66 Y.H. Deng, Y. Cai, Z.K. Sun, J. Liu, C. Liu, J. Wei, W. Li, Y. Wang and D.Y. Zhao, *J. Am.Chem. Soc.*, 2010, **132**, 8466-8473.
- 67 V. Ahmed, J. Kumar, M. Kumar, M.B. Chauhan, P. Dahiya and N.S. Chauhan, *J. Exp. Nanosci.*, 2015, **10**, 718-728.
- 68 M. Zarei, *Tetrahedron* 2013, **69**, 6620-6626.
- 69 J. Javidi, M. Esmailpour and M. Rajabnia Khansari, *RSC Adv.*, 2015, **5**, 73268-73278.
- 70 M. Esmailpour, J. Javidi and M. Zandi, *Mater. Res. Bull.*, 2014, **55**, 78-87.
- 71 C. Yang, J. Wu and Y. Hou, *Chem. Commun.*, 2011, **47**, 5130.
- 72 J. Yang, D. Wang, W. Liu, X. Zhang, F. Bian and W. Yu, *Green Chem.*, 2013, **15**, 3429-3437.
- 73 M. Esmailpour, J. Javidi, M. Mokhtari Abarghoui and F. Nowroozi Dodeji, *J. Iran. Chem. Soc.*, 2014, **11**, 499-510.
- 74 J. Wang, S. Zheng, Y. Shao, J. Liu, Z. Xu and D. Zhu. *J. Colloid. Interf. Sci.*, 2010, **349**, 293-299.
- 75 Clinical and Laboratory Standards Institute. *Methods for Dilution Antimicrobial Susceptibility Tests for Bacteria That Grow Aerobically; Approved Standard M7-A7*; Clinical and Laboratory Standards Institute: Wayne, PA, USA, 2006.
- 76 B. Das, M. Mandal, A. Upadhyay, P. Chattopadhyay and N. Karak, *Biomed. Mater.*, 2013, **8**, 035003.
- 77 J.A. Lemire, J.J. Harrison and R.J. Turner, *Nat. Rev. Micro.*, 2013, **11**, 371-384.
- 78 M. Esmailpour, A.R. Sardarian and J. Javidi, *Appl. Catal A: Gen.*, 2012, **445-446**, 359-367.
- 79 F. Dehghani, A.R. Sardarian and M. Esmailpour, *J. Organomet. Chem.*, 2013, **743**, 87-96.

Synthesis and characterization of β -lactam functionalized superparamagnetic $\text{Fe}_3\text{O}_4@\text{SiO}_2$ nanoparticles as an approach for improvement of antibacterial activity of β -lactams

Mohsen Esmailpour⁽¹⁾, Ali Reza Sardarian^{(1)*}, Aliasghar Jarrahpour⁽¹⁾, Edris Ebrahimi⁽¹⁾, Jaber Javidi^(2,3)



Preparation of magnetic β -lactam functionalized $\text{Fe}_3\text{O}_4@\text{SiO}_2$ nanoparticles has a synergic effect to improve the antibacterial activity.